16th World Conference on Earthquake, 16WCEE 2017

Santiago Chile, January 9th to 13th 2017

Paper N° 451

Registration Code: S-XXXXXXXX

IMPROVING ACCURACY OF THE SIMPLE ROCKING MODEL OF RIGID BLOCKS

D. Kalliontzis[(1)], S. Sritharan[(2)], A. E. Schultz[(3)]

[(1)] *Ph. D. student in the Dept. of Civil, Envir. & Geo-Eng., Univ. of Minnesota, Twin Cities, Minneapolis 55455, kalli072@umn.edu*

[(2)] *Wilson Engineering Professor in the Dept. of Civil, Constr. & Envir-Eng., Iowa State Univ., Ames 50011, sri@iastate.edu*

[(2)] *Professor in the Dept. of Civil, Envir. & Geo-Eng., Univ. of Minnesota, Twin Cities, Minneapolis 55455, schul088@umn.edu*

Abstract

In the Chilean earthquake in 1960, survival of several slender tall structures was attributed to their ability to respond in a rocking mode when experiencing the ground motion. Three years later, Housner developed a simple rocking model (SRM) to analytically explain the stability induced by rocking. The SRM was based on a planar rigid block pivoting on a rigid base about its bottom corners with the only source of damping being the impact energy loss. Since then, researchers have compared the SRM with experimental results of several geometrically different free-standing blocks. Their findings indicated that the SRM consistently overestimates the impact energy loss. Recognizing that the actual pivot point of a planar rocking block resides within its contact length with the base, this issue is addressed in this paper by accordingly modifying the SRM formulas. Comparisons with experimental data show that the proposed method significantly improves correlation to the measured coefficient of restitution (i.e., damping due to impact) compared to Housner's model.

Keywords: Rocking; Impact damping; Structures; Earthquake; Coefficient of Restitution

1. Introduction

To explain the stable response experienced by "golf-ball-on-a-tee" type of structures during the Chilean earthquake in 1960, Housner investigated their dynamic motion characteristics analytically using a simple rocking model (SRM) [1]. As shown in **Fig. 1**, the SRM portrayed a rigid rectangular block pivoting on a rigid base about its bottom corner (i.e., point O or O'). When $\theta > 0$, the block exhibits planar rocking motion, and when $\theta \rightarrow 0$, it impacts with the base. During an impact, part of its kinetic energy is dissipated and the energy loss is expressed using a coefficient of restitution (COR) term. Housner computed the COR corresponding to a rocking impact assuming conservation of angular momentum to hold between the moments just before and just after impact. Accordingly, the COR is computed as follows:

$$r = \left(\frac{\dot{\theta}_2}{\dot{\theta}_1}\right)^2 = \left[1 - \frac{MR^2}{I_o}(1-\cos(2a))\right]^2 \tag{1}$$

where $\dot{\theta}_2$ and $\dot{\theta}_1$ are the block angular velocities just after and just before impact, respectively; M denotes the block mass; R is the lever arm connecting its center of gravity with the pivot point; a is the angle characterizing the block slenderness, as shown in **Fig. 1**; and I_o is the mass moment of inertia of the block with respect to its pivot point.

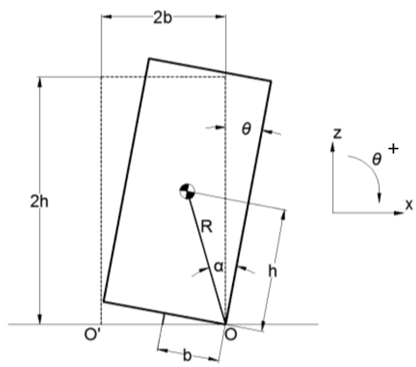

Fig. 1 – A free-standing rocking block as described by Housner (1963).

In case of a rectangular block, Eq. 1 can be simplified to Eq. 2 using $I_o = \frac{4}{3}MR^2$.

$$r = \left[\frac{1+3\cos(2a)}{4}\right]^2 \tag{2}$$

The accuracy of Eqs. 1 and 2 has been tested by several researchers using experiments of rocking blocks of various dimensions and different materials for the rocking block and base. Their experimentally obtained r values are compared with the SRM estimates in **Table 1**. The table shows Eqs. 1 and 2 to consistently underestimate the experimental values, while the differences between experiments and theory decrease with increase in the block slenderness ratio, *h/b*. Moreover, comparisons of tests from different researchers reveal that blocks with identical slenderness can exhibit discrepancies in r (e.g., experiment 2^a versus 2^b and 4^f versus 4^g); these disagreements may be associated with the use of different interface materials, or errors induced in sampling of experimental data. Nevertheless, as seen in the far right hand column of **Table 1**, the theoretical estimates are in all comparisons lower than the experimental records except for the most slender block (i.e., when *h/b* = 8.33).

Table 1 – Comparison of experimental *r* values and estimates by the SRM.

Slenderness ratio, *h/b*	Block & base materials	r_{SRM}	$r_{experiment}$	$r_{experiment} / r_{SRM}$
2[a]	Wood & steel	0.49	0.62	1.27
2[b]	Concrete & aluminum	0.49	0.76	1.55
2.85[e]	Granite & granite	0.70	0.86	1.23
3[a]	Wood & steel	0.72	0.77	1.07
4[a]	Wood & steel	0.83	0.88	1.06
4[c]	Concrete & steel	0.83	0.86	1.03
4[e]	Granite & granite	0.83	0.88	1.05
4[f]	Wood & aluminum	0.83	0.90	1.09
4[g]	Steel & steel	0.83	0.85	1.03
4.33[d]	Steel & wood	0.89	0.92	1.04
5.88[e]	Granite & granite	0.92	0.95	1.03
8.33[e]	Granite & granite	0.96	0.96	1.00

[a]Ogawa [2], [b]Priestley et al. [3], [c]Aslam et al. [4], [d]Muto et al. [5], [e]Peña et al. [6], [f]Fielder et al. [7], and [g]Lipscombe [8].

To improve estimation of *r* of rocking blocks, this study modifies the SRM formulas based on new experiments, which suggest that locations of pivot points just before and just after impact are away from the bottom corner. With an improved location for the pivot points, this paper introduces modified formulas (designated as MSRM) to obtain more accurate *r* values. This approach is then verified using the above-referenced tests, and comparisons with new test data of free-standing and controlled rocking blocks. Based on these comparisons, the MSRM is shown to significantly reduce the error between theoretical and experimental estimates.

2. Modified SRM formulas

In contrast to the SRM assumption of a rigid block having a single contact point with the base, recent findings have indicated that an actual rocking member establishes contact with its base over a finite length [9, 10, and 11]. Assuming that rotation occurs with respect to a point within the contact length, a different formulation for the coefficient of restitution is developed. Accordingly, the rotation centers just before and just after impact are located at some distance $\bar{b}$ from the centerline of the block, as shown in **Fig. 2**. Using Housner's assumption of conservation of angular momentum during an impact, an improved formula for *r* is derived based on this rocking configuration. The MSRM formula, as detailed in Eq. 3, depends on parameter *k*, which is equal to $\bar{b} / b$.

$$r = \left[\frac{1 + \frac{MR^2}{I_{cm}} \left(1 - (\sin a)^2 (1 + k^2)\right)}{1 + \frac{MR^2}{I_{cm}} \left(1 - (\sin a)^2 (1 - k^2)\right)} \right]^2 \tag{3}$$

where I_{cm} denotes the mass moment of inertia of the rocking member about its center of mass. Note that when $k = 1$ and by substituting $I_o = I_{cm} + MR^2$, Eq. 3 reduces to Eq. 2. For rectangular blocks, Eq. 3 can be simplified to Eq. 4.

$$r = \left[\frac{4 - 3(\sin a)^2 (1 + k^2)}{4 - 3(\sin a)^2 (1 - k^2)} \right]^2 \tag{4}$$

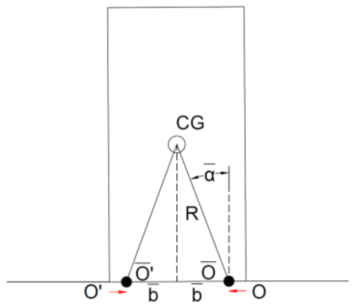

Fig. 2 – Rocking block at $\theta \rightarrow 0$ with its rotation centers just before and just after impact located within the block's contact length with the base; where $\bar{b}$ = kb and $0 \leq k \leq 1$.

3. Experimental estimation of parameter *k*

Test setup

Experimental data of three free-standing concrete rocking blocks were used to estimate an appropriate *k* value, based on the locations of their rotation centers just before and just after impact. The three units are presented in **Fig. 3** and include: a) a reinforced concrete square column with an added mass block with planar dimensions of 127 x 30.48 (width x height) cm^2 having its CG at 59.69 cm below the column's top face; b) the square concrete column with no added mass (Members 1a and 1b); and c) a reinforced concrete rectangular wall (Member 2). Properties related to the rocking behavior of the three members are presented in **Table 2**.

(a) Member 1a (b) Member 1b (c) Member 2

Fig. 3 – The three rocking units of the experimental investigation.

Table 2 – Properties of the three rocking concrete members.

Rocking member	*M*, kg	*R*, cm	**α*	Z_{CG}, cm	***p*, rad/s
1a	1,611.2	101.5	0.18	99.95	2.86
1b	542.9	85.6	0.21	83.82	2.93
2	963.2	126.4	0.29	121.28	2.41

**α* is estimated with respect to the Z_{CG}, which represents the height of the mass center.

**p denotes the dynamic parameter of a rocking block that is equal to $\sqrt{MgR / I_o}$.

All three members were excited in free vibration at three levels of initial top lateral drift (ITLD): 1%, 2% and 3%. Instrumentation for these tests included a series of light emitting diodes (LED), as shown in **Fig. 4**. More details on the test procedure are available in Kalliontzis and Sritharan [11] and Kalliontzis et al. [12].

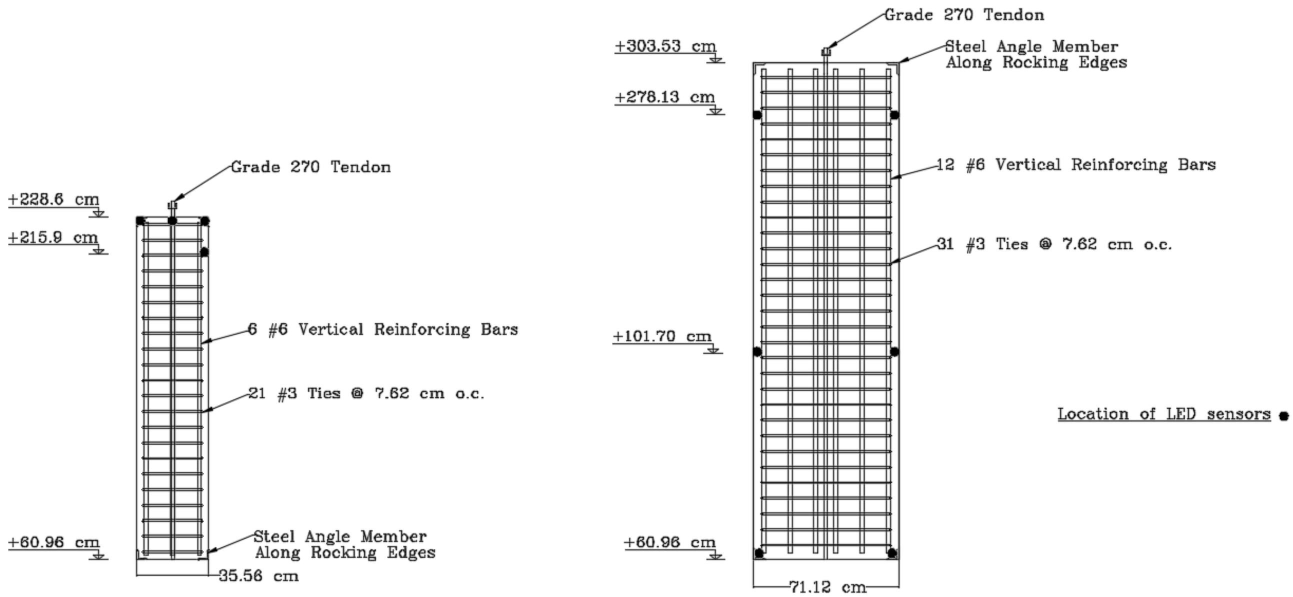

(a) Member 1a (b) Member 2

Fig. 4 – Reinforcement details and placement of LED sensors for Members 1a and 2. Similar details were used for Member 1b.

Estimating k

Experimental data from the aforementioned investigation is used to compute the rotation center locations just before and just after impact. This is done by assuming that an impact phase starts at the incipient instant of impulsive action, which is recorded in the experiments, and ends at its termination. As shown in **Fig. 5**, the impulsive response due to impact can be clearly found in the experimental linear acceleration data series. Showing this data for Members 1a and 2 for six consecutive impacts, the figure exemplifies how the moments just before and just after impact were selected.

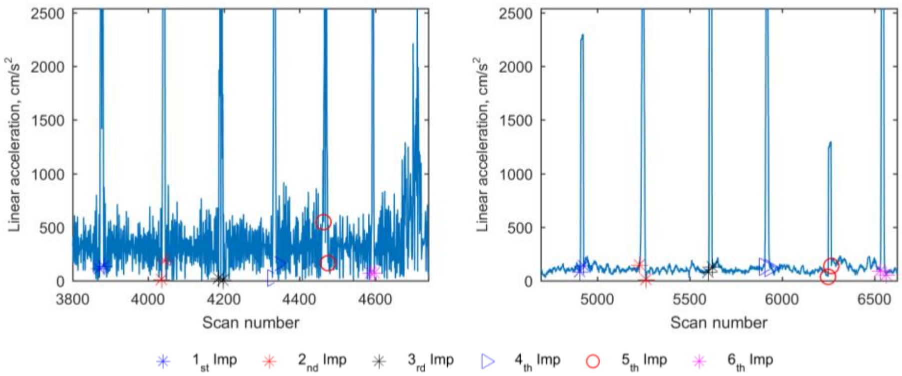

Fig. 5 – Experimental linear accelerations and points indicating the moments just before and just after impact; where Imp denotes impact.

Next, the correct rotation center for a chosen time instant is determined as the point at the rocking base that produces the closest agreement among the angular velocities calculated for all LED sensors of each member. **Fig. 6** presents these estimates for the previously shown impacts of Members 1a and 2, along with the corresponding points indicating the rotation center locations just before and just after impact (i.e., marked with bold circles). The figure reveals that the rotation center of a rocking member remains relatively constant at one side of its base before impact. Approaching an impact, it quickly migrates toward the opposite side, and once the impact phase ends, it stabilizes to a new position.

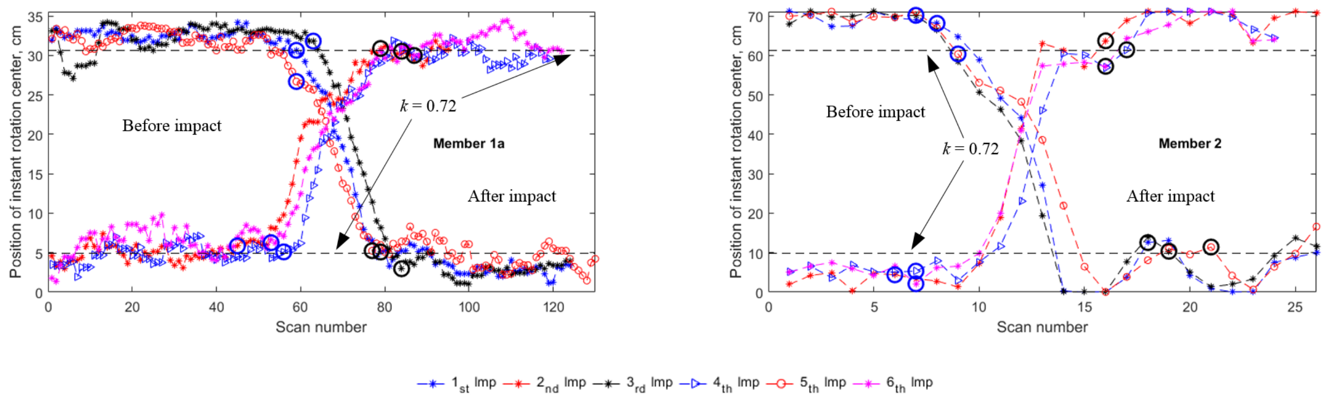

Fig. 6 – Rotation center motion along the member base before and after impact along with points indicating rotation centers just before and just after impact.

Using the information in **Fig. 6**, *k* values of the experimentally established rotation centers just before and just after impact are computed and presented in **Table 3**. The table shows that there is no significant variation between the three members regarding their experimental average *k* values. Therefore, for practical purposes, selecting a constant *k* to be equal to the average of all *k* values shown in this table is considered to be an adequate approximation. Accordingly, the computed $k = 0.72$ and the corresponding rotation center locations are included in **Fig. 6** using horizontal dashed lines, as shown.

Table 3 – *k* values obtained from experimental results, where N and S denote the north and south member sides.

	k value						
Rocking member	*1st* Imp	*2nd* Imp	*3rd* Imp	*4th* Imp	*5th* Imp	*6th* Imp	Experimental Average
1a, N	0.723	0.737	0.790	0.718	0.687	0.502	0.693
1a, S	0.714	0.670	0.834	0.714	0.705	0.647	0.714
1b, N	0.721	0.676	0.766	0.813	0.594	0.703	0.712
1b, S	0.644	0.623	0.705	0.546	0.826	0.666	0.668
2, N	0.916	0.792	0.973	0.728	0.698	0.610	0.786
2, S	0.647	0.876	0.709	0.850	0.679	0.722	0.747

4. Experimental Verification

Past data of free-standing rocking members

Fig. 7 presents comparisons between Eq. 2 by the SRM, Eq. 4 by the MSRM with k = 0.72, and the experimental data reported in **Table 1**. Comparing the two models, their estimates increasingly deviate with decrease in slenderness ratio. For the range of slenderness ratios tested by previous researchers, a better representation of the experimental trend is achieved by the MSRM, which significantly reduces the error difference between theoretical estimates and the recorded r values. For example, the largest error difference of about 55%, estimated using the SRM for the test by Priestley et al., is reduced to 9% using the MSRM, while, an error of about 23% for the test by Pena et al. with h/b = 2.85 decreases to 3.4%.

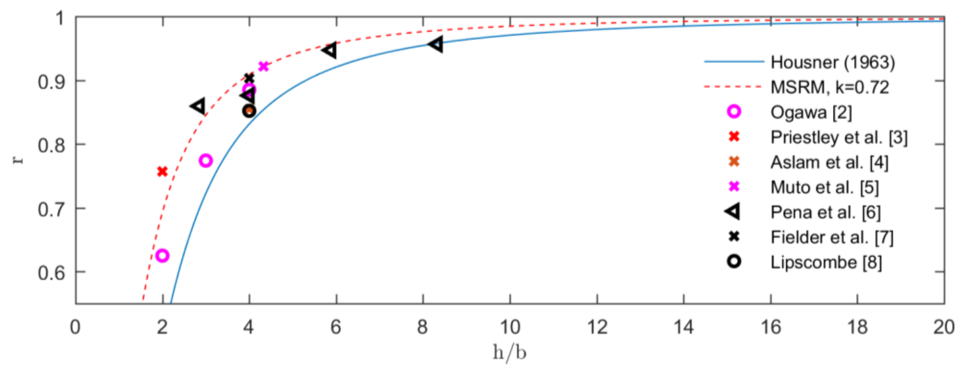

Fig. 7 – Comparison of past experiments with theoretical estimates by the SRM and MSRM with k = 0.72.

New data of free-standing rocking members

The experimental r values computed for the above-described three rocking members are plotted with respect to the approaching impact angular velocities for both the positive and negative directions in **Fig. 8**. Included in this figure are the theoretical estimates by the SRM and MSRM with k = 0.72. The figure shows the experimental values to fluctuate closely to the theoretical estimates by the MSRM. While, some data scatter is shown to occur for the lower velocity levels due to either noise effects in the velocity data, or imperfections in the rocking members. Nevertheless, no apparent deviation in r with respect to the ITLD can be observed in **Fig. 8** and this becomes clearer in **Table 4**, showing similar average r values regardless of ITLD (i.e., 1%, 2%, and 3%) for each of the three rocking members.

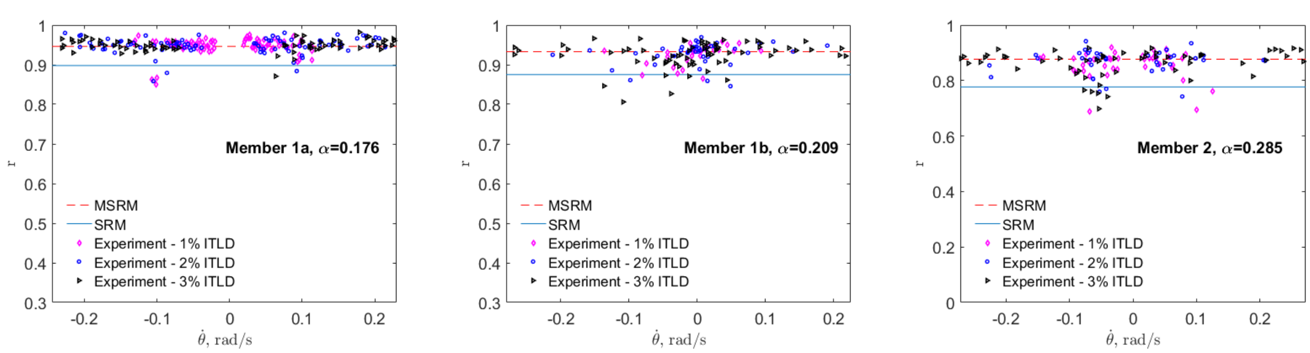

Fig. 8 – Comparison of new experiments with theoretical estimates by the SRM and MSRM with k = 0.72.

Table 4 – Experimental average r values with respect to the ITLD.

Rocking member	1%	2%	3%
1a	0.95	0.95	0.95
1b	0.92	0.93	0.93
2	0.86	0.87	0.86

Next, all points reported in **Fig. 8** are used to compute the overall average values of r and provide their comparisons with the theoretical predictions in **Table 5** (where the latter values are designated as r_{SRM} and r_{MSRM} for the SRM and MSRM, respectively). The table also includes the corresponding standard deviations, σ, coefficients of variation, C_v, and number of rocking impacts recorded for each member. Overall, the MSRM predictions agree well with the experimental means, while the SRM estimates are 6 to 11% lower than these values.

Table 5 – Experimental overall average r values and related measurements with respect to theoretical predictions

Rocking member	# of impacts	Experimental Average r	σ	C_v	r_{SRM}	$r_{\mathrm{exp}}/r_{\mathrm{SRM}}$	r_{MSRM}	$r_{\mathrm{exp}}/r_{\mathrm{MSRM}}$
1a	256*	0.95	0.019	0.020	0.90	1.06	0.95	1.00
1b	135	0.93	0.029	0.032	0.88	1.06	0.93	1.00
2	139	0.86	0.047	0.055	0.78	1.11	0.88	0.98

*Member 1a was subjected to a larger number of tests than the other members.

New data of controlled rocking members

In addition to free-standing member tests, this investigation used Members 1a and 2 to conduct free vibration tests of controlled rocking response. Accordingly, the two members were anchored to the foundation using an unbonded seven-wire tendon of 15.2 mm diameter (270 Grade) with an unbonded length of about 2.1 m and 2.8 m, respectively. Next, several tests were conducted with the tendon being post-tensioned to different force levels. Their values, as recorded from a load cell placed on top of the member, are presented in **Table 6**. A test setup similar to the free-standing member tests was used with ITLDs of 1 to 3% [11].

Table 6 – Initial post-tensioning forces (F_{PT}) used for the two rocking members.

Rocking member	F_{PT}, kN					
1a	0	2.22	12.45	24.46	40.03	48.04
b	0	17.8				

The experimentally computed r values are presented in **Figs. 9-10** for all cases in **Table 6** and compared with the theoretical estimates by the SRM and MSRM using k = 0.72. Similar to observations made in **Fig. 8**, the experimental data is shown to slightly fluctuate within a short range of values with the MSRM better capturing their r values compared to the SRM. This is confirmed in **Table 7**, which presents the mean r values of all controlled rocking tests. Based on these estimates, the MSRM well represents the average impact energy loss in the two controlled rocking members.

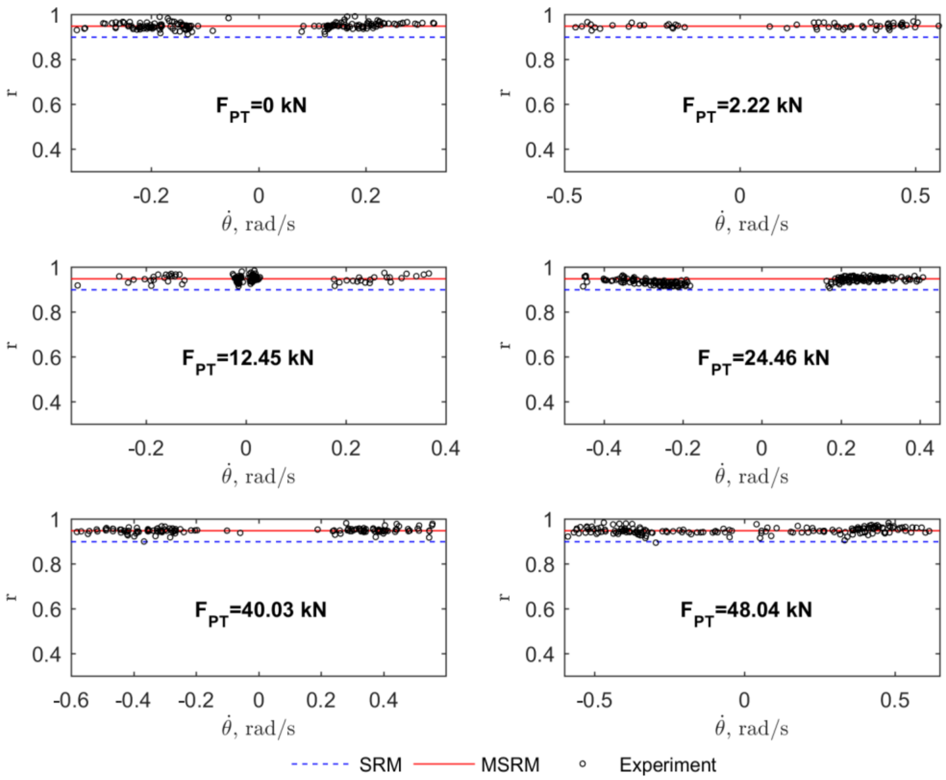

Fig. 9 – Comparison of controlled rocking tests of Member 1a with theoretical estimates by the SRM and MSRM using k = 0.72.

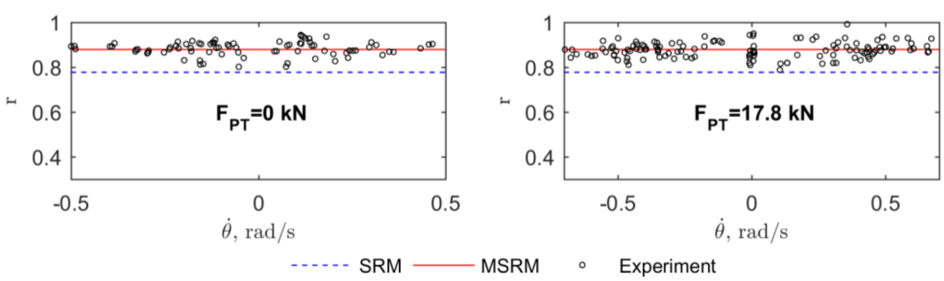

Fig. 10 – Comparison of controlled rocking tests of Member 2 with theoretical estimates by the SRM and MSRM using k = 0.72.

Table 7 – Average *r* values of controlled rocking tests compared with theoretical predictions by the MSRM using k = 0.72.

	F_{PT}, kN	r_{SRM}	r_{MSRM}	Average r_{exp}
Member 1a	0	0.90	0.95	0.95
	2.22	0.90	0.95	0.95
	12.45	0.90	0.95	0.95
	24.46	0.90	0.95	0.94
	40.03	0.90	0.95	0.95
	48.04	0.90	0.95	0.95
Member 2	0	0.78	0.88	0.88
	17.8	0.78	0.88	0.88

5. Conclusions

This paper revisited Housner's model of *r* and used past data of free-standing rocking blocks to evaluate its accuracy. This model has been reported to consistently underestimate the experimental records with their error difference increasing with decrease in slenderness ratio and the maximum error being as high as 55% in a test with h/b = 2. With a goal of improving modelling of *r*, a more realistic rocking configuration was assumed where a block rotates with respect to points that are away from its bottom corners. Estimates of the locations of these points were obtained experimentally based on new data from free vibration rocking tests of three free-standing concrete members.

Using these estimates and by following the conservation of angular momentum assumption made by Housner, modified formulas of *r* were derived (MSRM). The MSRM was then verified using data from three test sets, which included: a) the aforementioned past records of free-standing rocking blocks; b) the new records of three free-standing concrete rocking members; and c) new controlled rocking experiments, which used two of the latter members supplemented with an unbonded post-tensioning tendon and subjected to various initial force levels.

The MSRM improved comparisons with past tests having their maximum error difference decreased to 9%. New tests showed that *r* tends to vary within a short range of values for a given rocking member. The SRM was found to consistently underestimate these values in most cases. On the other hand, the MSRM effectively captured the experimental behavior, as it agreed well with the experimental *r* means in all of the free-standing and controlled rocking tests.

6. Acknowledgements

The work presented in the paper was undertaken as part of the "NEES Rocking Wall" project, with funding from the National Science Foundation (NSF) under Grant No. 1041650 and Precast/Prestressed Concrete Institute (PCI). Any opinions, findings and conclusions or recommendations expressed in this material are those of the authors and do not necessarily reflect the views of NSF or PCI.

7. References

[1] Housner GW (1963): The behavior of inverted pendulum structures during earthquakes. *Bull. Seismol. Soc. Am.*, **53** (2), 403-417.

[2] Ogawa N (1977): A study on rocking and overturning of rectangular columns. *Report of the Nat. Research Center for Disaster Prevention* (18), 14.

[3] Priestley MJN, Evison RJ, Carr AJ (1978): Seismic response of structures free to rock on their foundations. *Bull. New Zealand Nat. Soc. Earthquake Eng.*, **11** (3), 141-150.

[4] Aslam M, Salise DT, Godden WG (1980): Earthquake rocking response of rigid bodies. *J. Struct. Div.*, **106** (2), 377-392.

[5] Muto K, Umemura H, Sonobe Y (1960): Study of the overturning vibrations of slender structures. *Proc. 2nd World Congr. Earthquake Eng., Tokyo, Japan*, 1239-1261.

[6] Peña F, Prieto F, Lourenco PB, Campos Costa A, Lemos JV (2007): On the dynamics of rocking motion of single rigid-block structures. *Earthquake Eng. Struct. Dyn.*, **36** (15), 2383-2399.

[7] Fielder WT, Virgin LN, Plaut RH (1997): Experiments and simulation of overturning of an asymmetric rocking block on an oscillating foundation. *Eur. J. Mech. Solids*, **16** (5), 905-923.

[8] Lipscombe PR (1990): Dynamics of rigid block structures. *Ph. D. Thesis*, University of Cambridge, U. K.

[9] Aaleti S, Sritharan S (2009): A simplified analysis method for characterizing unbonded post-tensioned precast wall systems. *Engineering Structures*, **31** (12), 2966-2975.

[10] Ma QTM (2009): The mechanics of rocking structures subjected to ground motion. *Ph. D. Thesis*, The University of Auckland, New Zealand.

[11] Kalliontzis D, Sritharan S (2014): A finite element approach for modelling controlled rocking systems. *2nd Eur. Conf. Earthquake Eng. Seism.*, Istanbul, Turkey.

[12] Kalliontzis D, Sritharan S, Schultz AE (2016): Improved coefficient of restitution estimation for free rocking members. *J. Struct. Eng.*, 10.1061/(ASCE)ST.1943-541X.0001598, 06016002.